IMPURITIES IN MAGNETIC CRYSTALS

L. Pál

The paper is an exposition of modern ideas about the magnetic structure of dilute alloys, the electric and magnetic screening of impurities, and the distortion of the magnetic moment distribution in the matrix due to impurity atoms. A review is also given of the experimental methods of studying the effect of impurities on the magnetic properties of iron and other magnetic materials. The main attention is devoted to neutron diffraction methods, by means of which the magnetic moment distribution in an alloy and the magnetic form factors can be studied. The last section is concerned with the effect of the matrix on the impurity energy levels, and the results are given of neutron experiments on virtual and localized levels that arise in a magnetic material when impurities are present.

INTRODUCTION

The preparation of especially pure materials is intimately related to the study of impurities; for to avoid or exploit the effect of impurities on the properties of a material, one must know the intrinsic physical properties of the impurities. There is another, purely theoretical reason why the problem of impurities is attracting ever greater attention. Impurity atoms, which can be regarded as test bodies of atomic dimensions, perturb the matrix formed by the host component; the nature of this perturbation depends strongly on the most important characteristics of the pure matrix – the impurities make the properties of the host materials amenable to investigation. For example, the electron structure of the impurity atoms is changed to a greater or lesser extent by the interaction with the matrix atoms; study of the change yields much useful information for theoretical physics.

This review is concerned with the effects of impurities on the magnetic properties of materials. The subject is difficult, involving aspects of the problem of impurities as a whole that have not yet been fully resolved. The main difficulty is that the electronic structure of the most important magnetic materials is not sufficiently well studied; overcrude simplifications must be used to explain a number of effects. Other difficulties arise from the absence of a satisfactory theory of magnetism in metals.

Basically, we shall discuss iron with transition-element impurities. We shall assume that each impurity atom and the region it affects are unperturbed by other impurity atoms, which must therefore have a low concentration, though there is, of course, no general criterion of a high or low concentration, this depending on the interaction between the impurities and the matrix.

Our first topic is the perturbation of the electric charge and the magnetic moment in an individual impurity atom and its neighboring atoms. The second topic is more complicated; it is connected with the violation of translational symmetry in the crystal. The energy level scheme is greatly complicated by this perturbation because the quasimomentum – a good quantum number for excitations in a perfect crystal – is not conserved when impurities are present; isolated levels can be formed above the quasicontinuous energy band, and the density of states is affected.

Central Institute of Physical Investigations, Hungary. Translated from Problemy Fiziki Élementarnykh Chastits i Atomnogo Yadra, Vol. 2, No. 4, pp. 1003-1027, 1972.

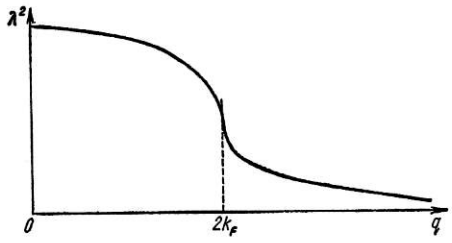

Fig. 1. Screening parameter as a function of the wavelength.

We shall not discuss the problem of the localization of a magnetic moment, although it is closely related to the first topic. A fairly simple formalism is capable of describing the perturbation of the electric charge and the magnetic moment and we can directly study the changes that occur in the matrix when impurities are introduced.

SCREENING OF CHARGE AND SPIN

The classical Debye–Huckel theory for strong electrolytes showed that the charge of the positive ions is screened by a cloud of negative ions. The same thing happens in metals if one of the host atoms is replaced by an impurity atom with a different ion charge. The perturbation due to the difference of the ion charges is screened by electrons of both spin directions so that the spin density does not change if there are no exchange effects. The screening must be self-consistent; that is, the distribution of the electron charge must be such that the resulting local potential completely determines the local charge density. In the simplest case, the effective potential is equal to the well-known Debye–Huckel potential:

$$V_{\text{eff}}(s) = \frac{ze}{r} e^{-\lambda r}, \tag{1}$$

where z is the difference between the ion charges and

$$\lambda = e\sqrt{4\pi N(E_f)} \tag{2}$$

is the screening parameter. The characteristic screening radius, λ^{-1}, is inversely proportional to the Fermi momentum. If the density of states near the Fermi energy is high, the region in which the host atoms are perturbed is fairly small. In general, the potential has a more complicated form. The definition of the screening parameter can be generalized by means of the Fourier transform of the effective potential; for free electrons

$$\lambda^2 = \frac{4\pi e^2 n}{\frac{2}{3}E_f}\left\{\frac{1}{2} + \frac{4k_f^2 - q^2}{8k_f q}\ln\left|\frac{2k_f + q}{2k_f - q}\right|\right\}. \tag{3}$$

Here k_f and E_f are the Fermi momentum and energy, respectively, and n is the electron density. The screening parameter is shown as a function of the wavelength in Fig. 1. The effective screening radius, λ^{-1}, increases with p. The logarithmic singularity at $q = 2k_f$ leads to numerous experimentally observable anomalies; in particular, the screening becomes oscillatory, that is, the density of the screening charge is not a smooth function of the distance but exhibits oscillations with wave number $2k_f$.

This simple model must be generalized to systems in which the density of electron states at the Fermi energy is not the same for different spin orientations. In these systems impurity atoms perturb not only the charge density but also the spin density; the magnetic moment is changed at the impurity and at its neighboring sites.

These notions enable one to get a better understanding of the changes of the magnetic moments observed in iron that contains impurities of the transition elements. Now the Fermi surface of iron has a fairly complicated structure and it is difficult to use it directly for calculations. To describe the electron structure of iron at least approximately, I have therefore chosen a model of mixture of three gases; each consists of free electrons, but the Fermi energies of the gases are different.

Neutron scattering experiments show that an impurity atom's effect on the magnetic moment distribution depends strongly on its position – to the left or the right – relative to iron in the periodic table. In the simplest cases, the sign of the perturbing charge, ze, determines the sign of the change of the magnetic moment at the impurity site. Roughly speaking, the perturbing charge is proportional to the difference in the number of external electrons:

$$z = z(i) - z_0, \tag{4}$$

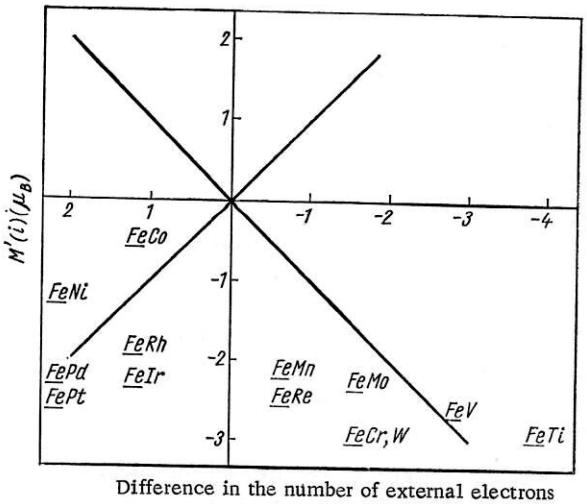

Fig. 2. Variation of the magnetic moment of an impurity site as a function of the difference in the number of external electrons [1].

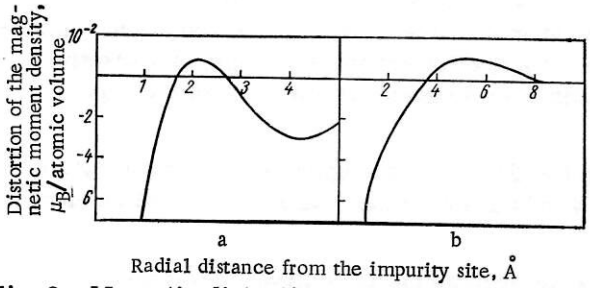

Fig. 3. Magnetic distortion produced by impurities to the left of iron in the periodic table: a) screening predicted by continuous model; b) screening deduced from experimental data [2].

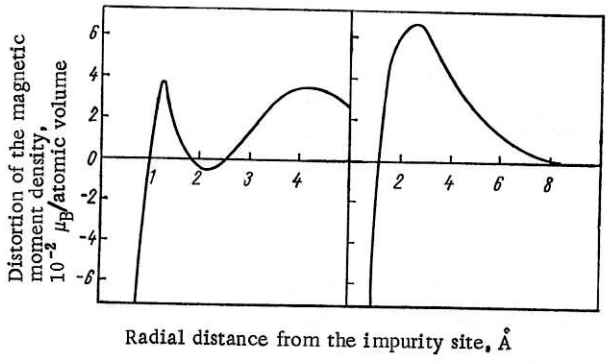

Fig. 4. Magnetic distortion due to impurities to the right of iron in the periodic table: a) predictions; b) experimental data [2].

where z(i) is the number of electrons outside the outermost closed shell of the neutral impurity atom and z_0 is the corresponding number for the host atom.

In Fig. 2, which is taken from [1], the change in the magnetic moment at an impurity site is plotted against z, the difference in the number of external electrons. The change in the magnetic moment is defined by

$$M'(i) = M(i) - M_0, \qquad (5)$$

where M(i) is the impurity's magnetic moment and M_0 the host atom's. The straight lines $M'(i) = \pm z(i)\,\mu_B$ correspond to the simplest case, which was considered by Friedel. Figure 2 shows that the experimental data depart strongly from these straight lines only for the impurities to the right of iron in the periodic table.

This elementary description can, of course, be improved by taking into account the screening of the charge and the exchange interaction between electrons with opposite spin projections.

In accordance with Low's calculations [2], a perturbation produced by a negative point charge, $z < 0$, causes the magnetic moment to be redistributed in the manner shown in Fig. 3. The screening electrons are repelled from a center with $z < 0$; since the majority of them have the predominant spin direction, a suppression of the magnetic moment is to be expected near the impurity. This agrees well with the experimental data – the moment decreases appreciably for impurity elements to the left of iron in the periodic table. However, it must be noted that, although the distortion of the magnetic moment density is initially negative, it becomes positive at large distances.

Low and Collins [3, 4] found good agreement when they compared their neutron scattering data with calculations of the magnetic moment distribution based on the above assumptions; however, there was a discrepancy – the radial scale of the theoretical curve in Fig. 3 is much less than that of the experimental curve.

Low attributed this discrepancy to the assumption of a continuous charge distribution: in a real crystal, the screening charge is induced in orbitals of atoms at discrete sites; continuity presupposes that the screening charge around an impurity is not localized at the lattice sites. There is another difference between the curves of Fig. 3; curve a, which describes screening in a continuous model, is oscillatory, while b, the experimental curve, indicates the presence of electron scattering by impurities, which suppresses the oscillations. However, this difference is not too serious, since the resolution in neutron scattering experiments is not adequate to observe structure on a scale of 2 Å in the magnetic moment

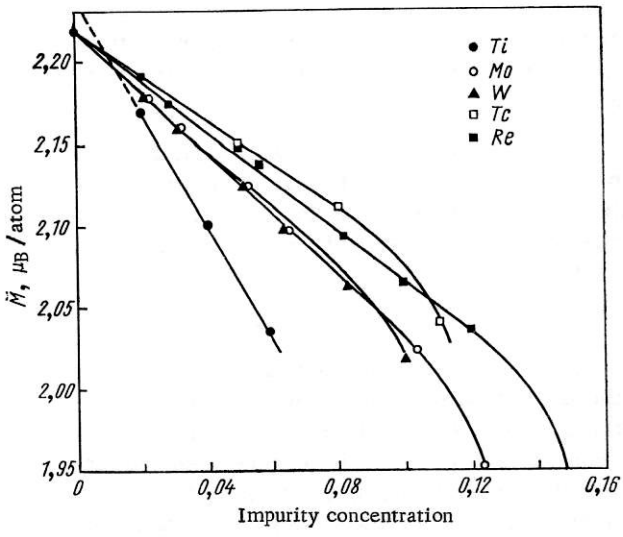

Fig. 5. Mean magnetic moment of iron as a function of the concentration for different impurities.

distribution; and in any case the oscillatory behavior predicted by Low's calculations could be due to the model – a free electron gas.

Figure 4 shows the results of calculations [2] for an attractive charge; that is, for impurities to the right of iron in the periodic table. The redistribution predicted by the electron-gas model is similar to that of a repulsive charge but with the opposite sign; the attractive charge increases the moment near an impurity site because the majority of the screening electrons have the predominant spin direction. However, the experiments show that the moments of many impurities to the right of iron decrease by $(0.5\text{-}2.0)\mu_B$.

The experimental results can be readily understood by noting that the number of holes in the band of the predominant spin direction in iron is very small and that the density of hole states near the Fermi level decreases very rapidly when the number of electrons with predominant spin increases. The orbitals with predominant spin at the impurity sites are unable to accept one or two additional screening electrons; in other words, electrons with spin upward are ineffective for the screening of attractive charges; the electrons with spin downward must play the main role, in good agreement with the experimentally observed tendency for the moment to decrease.

An increase in the magnetic moment is to be expected for the nearest neighbors of an impurity atom; experimentally, this is so, as follows from curve b in Fig. 4, which shows the magnetic moment redistribution for impurities to the right of iron.

In some cases the increase in the magnetic moment of the iron atoms is so great that it compensates the decrease in the moment at the impurity site.

EXPERIMENTAL METHODS

There are three main ways of studying the effect of impurities on the magnetic properties of iron or other magnetic metals experimentally: by measuring 1) the macroscopic magnetization; 2) the magnetic form factors by means of neutrons; 3) the hyperfine fields by means of nuclear magnetic resonance and the Mössbauer effect.

The macroscopic magnetization can be measured with an error of less than 0.1%, so that the mean magnetic moment $\bar{M}$ per atom can be determined quite accurately as a function of the concentration. The mean magnetic moment of iron as a function of the concentration is shown in Fig. 5, which is taken from [5], for different impurities. If the mean moment of the host and impurity atoms does not depend on the concentration, the measured mean moment is simply

$$\bar{M} = M_0 + [M(i) - \bar{M}_0]\, c. \qquad (6)$$

In many cases $\bar{M}_0$ is very near M_0, the magnetic moment of an atom of the pure metal. However, any change in the magnetic moment of the matrix atoms can lead to a deviation from $\bar{M}_0$.

Table 1 gives $\bar{M}_0$ and $M(i) - \bar{M}_0$ as calculated by means of the above simple expression for different dilute alloys with an iron matrix; the difference $M(i) - \bar{M}_0$ is negative for the majority of the impurities, in broad agreement with the proposed screening mechanism.

Measurement of the form factor by means of neutrons affords a powerful method of studying the magnetic moment distribution around an impurity atom. Slow neutrons, whose magnetic moments interact with the electron spins, are diffusely scattered and their distribution after scattering depends on the Fourier components of the magnetic moment distribution about the impurity atom. The expression for the differential cross section of elastic incoherent scattering of unpolarized neutrons was derived by various authors many years ago (see, for example, [3]):

TABLE 1

Impurity	$\overline{M}_0$	$\overline{M}'(i)$	Impurity	$\overline{M}_0$	$\overline{M}'(i)$
Ti	2,24	−3,39	Pd	2,22	−0,61
V	2,23	−3,29	Ta	2,17	−4,61
Cr	2,23	−3,76	W	2,22	−2,04
Mn	2,16	−1,64	Re	2,22	−1,56
Co	2,22	+1,14	Ir	2,23	+0,57
Mo	2,17	−2,15	Pt	2,22	+1,69
Rh	2,21	+1,04			

TABLE 2

Impurity	$M(i)$	$M(i)-M_0$	$\frac{d\overline{M}}{dc}=M(i)-\overline{M}_0$	Impurity	$M(i)$	$M(i)-M_0$	$\frac{d\overline{M}}{dc}=M(i)-\overline{M}_0$
Ti	−0,7	−2,9	−3,4	Rh	0,5	−1,7	1,0
V	−0,4	−2,6	−3,3	Pd	0,1	−2,1	−0,6
Cr	−0,7	−2,9	−3,8	W	−0,7	−1,5	−2,0
Mn	0,0	−2,2	−1,6	Re	−0,3	−1,9	−1,6
Co	2,1	−0,1	1,1	Os	0,0	−2,2	−1,6
Ni	0,9	−1,3	0,6	Ir	0	−2,2	0,6
Mo	−0,1	−2,3	−2,2	Pt	0	−2,2	1,7
Ru	0,9	−1,3	0				

$$\frac{d\sigma}{d\Omega}=\left(\frac{\gamma e^2}{2mc^2}\right)^2 Nc\,(1-c)\sin^2\alpha\left|\int m'(\mathbf{r})\,e^{i\mathbf{kr}}\,d^3r\right|^2, \tag{7}$$

where **k** is the scattering vector of the neutrons; α is the angle between **k** and the magnetization; m'(**r**) is the deviation of the density of the magnetic moment's z component at the point **r** from its value in a pure metal if an impurity atom is at **r** = 0; the term $\gamma e^2/2mc^2$ has the numerical value 0.073 b; N is the total number of atoms in the crystal. The forward scattering cross section (k = 0)

$$\frac{d\sigma}{d\Omega}=0{,}073Nc\,(1-c)\sin^2\alpha\left|\int m'(\mathbf{r})\,d^3r\right|^2 \tag{8}$$

depends directly on the rate of change of the mean magnetization with respect to the impurity concentration, i.e.,

$$\int m'(\mathbf{r})\,d^3r=\frac{d\overline{M}}{dc}. \tag{9}$$

If the mean magnetization is a linear function of the concentration, then

$$\frac{d\overline{M}}{dc}=M(i)-\overline{M}_0, \tag{10}$$

and this quantity is known for many dilute alloys from magnetization measurements. But the most important thing is that neutron scattering enables one to determine the distribution of the moments separately for the two components of an alloy; for m'(**r**) consists of two parts; one of them includes the magnetism of d electrons on the orbits at the impurity sites, the other the concentration from all the remaining sites; separating out explicitly the two parts in the scattering cross section and assuming that the magnetic moment around an impurity is redistributed in a spherically symmetric manner, we obtain

$$\frac{d\sigma}{d\Omega}=0{,}073Nc\,(1-c)\sin^2\alpha\,\{M'(i)\,f_i(k)+M'(h)\,f_h(k)\}^2, \tag{11}$$

where $f_i(k)$ and $f_h(k)$ are the form factors of the impurity and host atoms, respectively:

$$M'(i)=\int m_i'(\mathbf{r})\,d^3r \quad \text{and} \quad M'(h)=\int m_h'(\mathbf{r})\,d^3r. \tag{12}$$

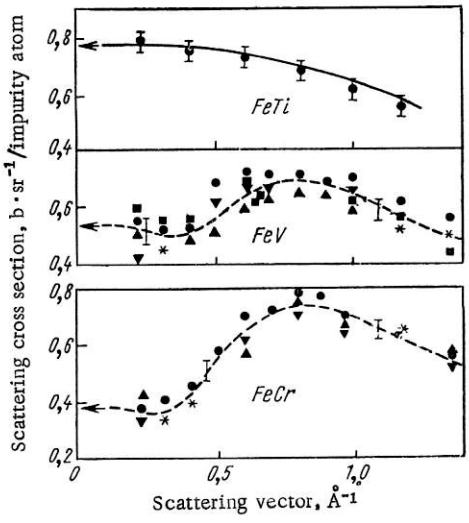

Fig. 6. Scattering cross sections [4] for Fe(Ti), Fe(V), and Fe(Cr) as a function of the scattering vector. The number of symbols along the curve of each alloy corresponds to the number of samples.

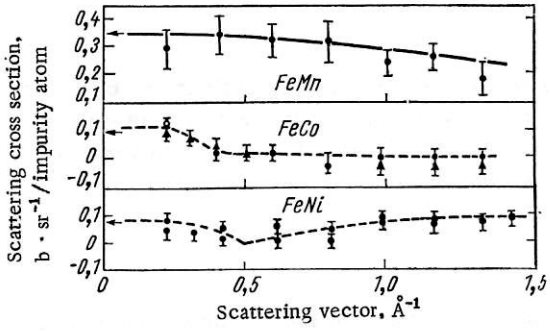

Fig. 7. Scattering cross sections [4] for Fe(Mn), Fe(Co), and Fe(Ni) as a function of the scattering vector. The number of symbols along the curve of each alloy corresponds to the number of samples.

Since $f_h(k)$ must tend to zero as k increases, it is not difficult to determine $f_i(k)$: the cross section must be measured for large k.

The cross sections measured by Collins and Low [4] are plotted against the scattering vector for different impurities in Figs. 6-9. A complete Fourier transformation is impossible – the range of k values in a real experiment is very limited – so that the magnetic moment redistribution cannot be found exactly. Nevertheless, much useful information can be extracted; the moment localized at the impurity atoms can be estimated, as we have already pointed out, from the behavior of the cross section at large k. Figure 10 compares the magnetic moments measured by Low and Collins [4] with those calculated by Campbell [6] for different elements; for comparison the values of $d\bar{M}/dc$ are also given in Table 2. It is true that no great accuracy can be claimed for the values of the impurity moments, but the difference between the values of $\bar{M}(i) - \bar{M}_0$ and $d\bar{M}/dc$ clearly indicates a strong change in the value of the magnetic moments of the host atoms around an impurity.

Following Collins and Low [4], let us consider how an iron atom is affected by the perturbation. The deviations of the mean moments of nearest neighbors from the moment of an atom of pure iron are given in Fig. 11 for different impurities. More detailed information about the perturbation can be obtained by analyzing the scattering cross-section data. Figure 12 shows the part of the scattering amplitude that corresponds to perturbations of the iron matrix as a function of the scattering vector for different impurities to the left of iron in the periodic table; the general form of the curve agrees with the theoretical predictions. In the upper part of the figure we show the hypothetical distortion of the magnetic moment density in coordinate space; the scattering amplitude that corresponds to this distribution is shown in Fig. 12 as a function of the scattering vector by the dashed line. As the hypothetical dependence differs in no essential respect from the experimental curves, it can be concluded that the perturbation of the magnetic moment density has a maximum at a distance of approximately 5 Å.

The scattering amplitudes that correspond to the perturbations of the matrix when the impurities are elements to the right of iron in the periodic table are shown in Fig. 13. Here there is an important difference. The upper diagram shows the hypothetical radial distribution of the magnetic moment density of iron atoms that surround an impurity atom; the main curves show the corresponding scattering amplitude as a function of the scattering vector. The similarity between the curves indicates that the perturbation of the magnetic moment density of the iron atoms is everywhere positive and does not oscillate as in the earlier case.

An attempt should be made to find a rigorous theoretical explanation of these experimental results. Unfortunately, we can adduce only heuristic arguments. The different perturbing effects of the two kinds of impurity can be explained by the position of the Fermi level in the electron d bands with spin up and down; for experimental data indicate that the spin-down band is filled to a deep minimum and the spin-up band to a low maximum on the density of states curve. If this is so, the difference in the nature of the screening of the spin density for the two classes of impurity is natural.

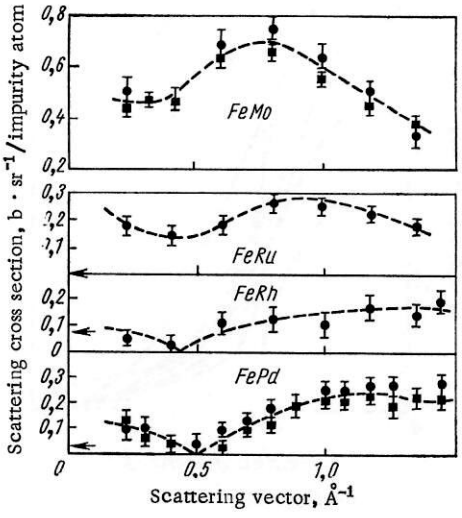

Fig. 8

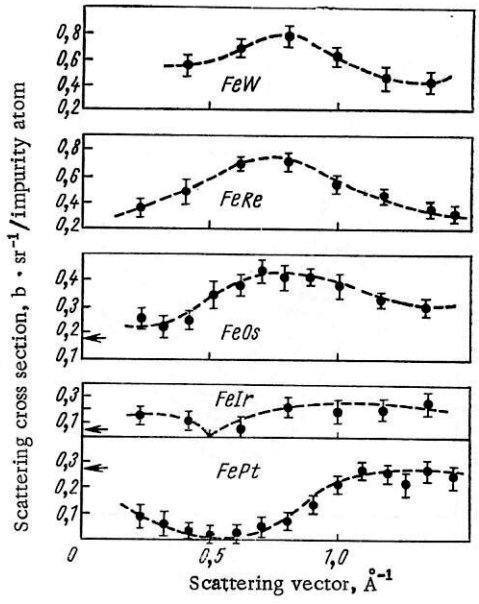

Fig. 9

Fig. 8. Scattering cross sections [5] for Fe(Mo), Fe(Ru), Fe(Rh), and Fe(Pd) as a function of the scattering vector. The number of symbols along the curve of each alloy corresponds to the number of samples.

Fig. 9. Scattering cross sections [4] for Fe(W), Fe(Re), Fe(Os), Fe(Ir), and Fe(Pt).

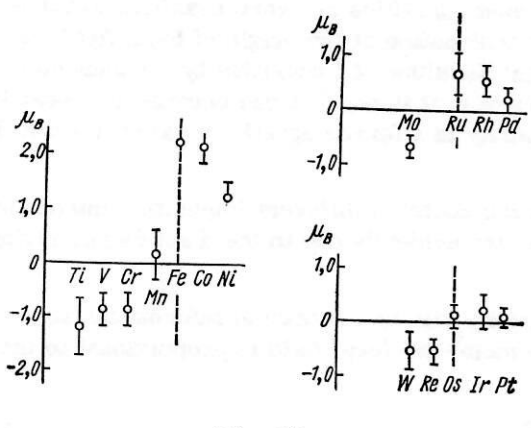

Fig. 10

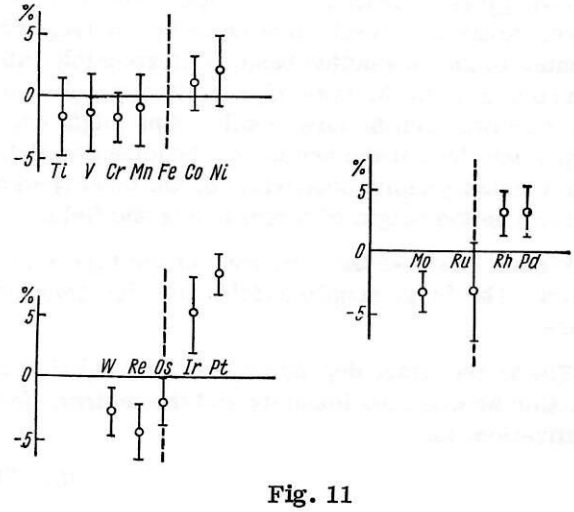

Fig. 11

Fig. 10. Impurity moments calculated by Campbell [6] for different elements.

Fig. 11. Deviation of the mean moment of nearest neighbors of an impurity from the moment of an atom for pure iron for different impurities [1].

A great deal of work has been done on the distortion of the hyperfine field by impurity atoms. The hyperfine field is very sensitive to small changes around the nucleus and its study provides much useful information for the understanding of magnetic properties of dilute alloys.

The hyperfine field in ferromagnetic metals is due primarily to two factors: 1) polarization of the inner s shell of the core by the magnetic moment of the d spin; 2) the change in the polarization of the electrons of the valence s conduction band by magnetized d spins.

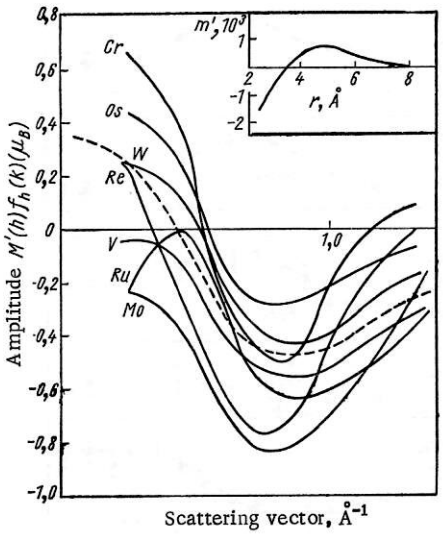

Fig. 12

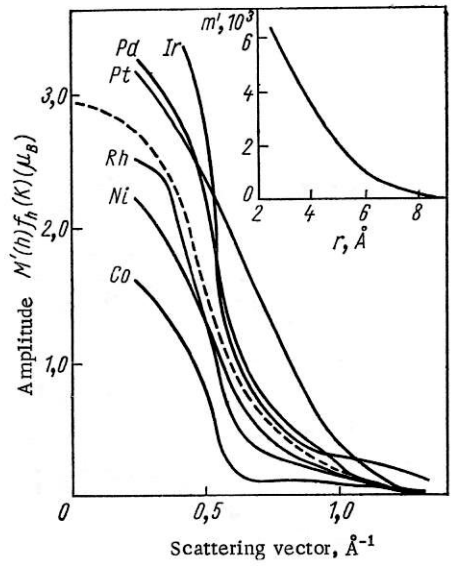

Fig. 13

Fig. 12. The part of the scattering amplitude that corresponds to perturbations of the iron matrix as a function of the scattering vector for impurity elements to the left of iron in the periodic table [4].

Fig. 13. As in Fig. 12, but for impurity elements to the right of iron in the periodic table [4].

The first gives rise to a hyperfine field whose direction is opposite to the magnetization of the d spins; the second gives a positive contribution, since the exchange interaction of s and d electrons is usually positive. However, an effective negative exchange interaction can arise because of the covalent admixture of d states in the conduction band. Unfortunately, all the relevant quantities are very sensitive to band-structure details in the case of transition metals, so that any explanation of the origin of local fields is very uncertain, even in pure metals. One might even think that the study of impurities by measurement of the hyperfine field at the nuclei is a hopeless undertaking; however, it is not that bad because the most important thermodynamic properties of the local field at an impurity in a ferromagnetic metal at T = 0°K do not depend on the origin of magnitude of the field.

Figure 14 shows the strengths of the hyperfine fields at the nuclei of different impurities introduced into iron. The large negative fields for the transition metals are evidently due to the d spin's polarizing the core.

The temperature dependence of the local field at an impurity site is a source of information about the interaction between the impurity and the matrix. In the pure metal the local field is proportional to the magnetization, i.e.,

$$H_{int}(T) = AM(T), \tag{13}$$

where A does not depend on the temperature. The temperature dependence of the local field may be completely different for impurity and host atoms. A good example is afforded by the results of Jaccarino et al. [7], for iron with manganese impurities; the temperature dependence of the reduced hyperfine field, $H'_{int}(T) \times [H'_{int}(0)]^{-1}$ is shown in Fig. 15. The temperature dependence of the reduced total bulk magnetization, $\sigma(Y)/\sigma(0)$, is shown for comparison. If it is assumed that the constant A_{imp} of the hyperfine field at the impurity is also independent of the temperature, and the exchange polarization of the conduction electrons is ignored,

$$\frac{H'_{int}(T)}{H'_{int}(0)} = \frac{\sigma_{imp}(T)}{\sigma_{imp}(0)} \tag{14}$$

TABLE 3

Impurities	Ti	V	Cr	Mn	Co
$\frac{100\Delta H_1}{H_0}$	—6,5	—7,6	—8,3	—6,8	+4,3
$\frac{100\,\Delta H_2}{H_0}$	—6,0	—6,4	—7,0	—1,0	+2,1

Note. H_0 = 330 kOe.

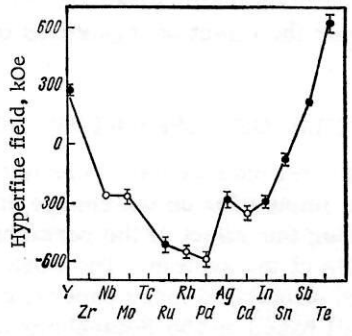

Fig. 14

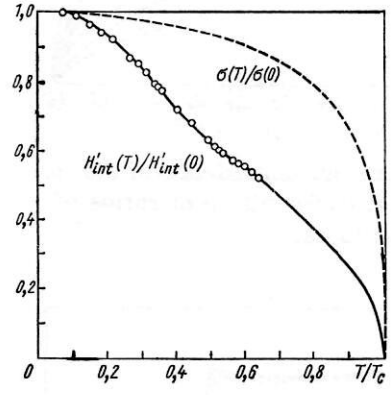

Fig. 15

Fig. 14. Hyperfine fields at the nuclei of impurities introduced into an iron matrix.

Fig. 15. Temperature dependence of the hyperfine field at an impurity in Fe(Mn) [7]. The temperature dependence of the reduced bulk magnetization is shown for comparison.

If only nearest neighbors are allowed for, $\sigma_{imp}(T)$ can be easily calculated in the molecular field approximation. Results of calculations are shown in Fig. 16; the form of the curve depends on the ratio of the exchange constants, that is, on the parameter $\varepsilon = J'/J$, where J' and J are the impurity-matrix and matrix-matrix exchange constants, respectively. It is clear that the weakly coupled moment of the impurity must decrease with increasing temperature much faster than the bulk moment of the material; this does happen in the case of iron with manganese impurities.

If the polarization of the conduction electrons is also allowed for, the expression for the local field takes on a new term, which is proportional to the bulk magnetization, i.e.,

$$H'_{int}(T) = A\sigma_{imp}(T) + B\sigma(T). \qquad (15)$$

The best agreement with the experimental curve of Jaccarino et al. is obtained if 16% of the magnetic field strength at the impurity is attributed to polarization of the conduction electrons and the ratio J'/J is taken to be 0.44.

The impurity atoms strongly perturb the hyperfine field at the nearest and next-nearest iron atoms; this has been established for many elements mixed with iron. One would expect the hyperfine field and the magnetic moment density to be equally distorted, but spin magnetism distributions calculated from the neutron scattering cross sections do not agree with those deduced from measurements of the hyperfine field.

Using usual methods of analysis, one can calculate the distortion of the hyperfine field at the nearest and next-nearest neighbors from the Mossbauer spectra. Table 3 contains the changes in the hyperfine

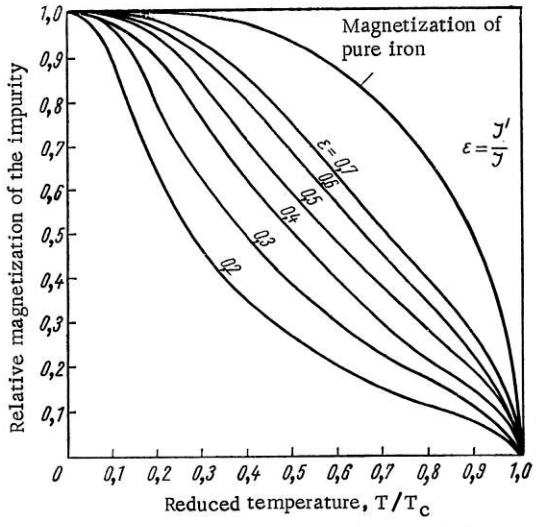

Fig. 16. Temperature dependence of the impurity magnetization for different ratios of the exchange constants.

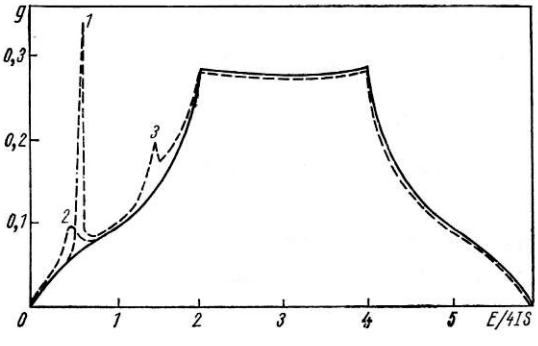

Fig. 17. Spin-wave spectrum calculated by Izyumov [9] for a simple cubic lattice with and without impurity atoms. The continuous curve is for a perfect crystal; the dashed curve, for one with an impurity: 1) $J'/J = 0.2$; $S'/S = 0.25$; 2) $J'/J = 0.2$; $S'/S = 4.0$; 3) $J'/J = 0.5$; $S'/S = 0.25$.

field when the most interesting impurities are present; with the exception of cobalt, all the impurities decrease the hyperfine fields at the iron nuclei in the first and second coordination spheres compared with the field in pure iron.

Although this agrees qualitatively with the density of the magnetic moment distribution obtained from neutron scattering experiments, the agreement is unsatisfactory; the neutron scattering experiments with Mn as impurity are consistent with the assumption that there is no localized moment at the impurity site, but measurements of the hyperfine field show conclusively that a localized moment is present. To obtain the deepest possible understanding of the magnetic moment distribution around an impurity atom, we must consider the effect of impurities on the energy levels.

LEVELS OF IMPURITY ATOMS

In the first part we have considered the effect of magnetic impurities on the charge and spin distributions, ignoring the effect of the perturbation on the energy levels of the system. The work of Wolfram and Callaway [8] stimulated many papers, but unfortunately they were all based on the Heisenberg model, which does not correspond best to metallic systems. True, this model may give a qualitative description of the perturbation of energy levels, but it must be regarded skeptically for the interpretation of more subtle effects.

As is well known, the magnetic moments in an ordered magnetic system execute coherent oscillations – spin waves – and these oscillations determine the temperature dependence of the magnetic susceptibility and the magnetic part of the specific heat. Scattering by the crystal of neutrons with suitable energies yields direct information about the energy levels of the spin waves. The energy of the spin waves has been measured as a function of the wave vector for many magnetic crystals. If an impurity atom is placed in a crystal, the frequency spectrum of the spin waves is perturbed. The nature of the perturbation is governed basically by two parameters; one of them is the ratio of the impurity-matrix and matrix-matrix exchange integrals, i.e., $\varepsilon = J/J'$; the other is the ratio of the spins of the impurity and host atoms, i.e., S'/S. Depending on the values of the parameters, the impurity levels may be localized or virtual.

The localized levels are situated outside the spin-wave band and cannot interact with the spin waves of the matrix. Therefore, the lifetime of the localized levels is determined by interactions that are not of a spin-wave nature. But the virtual levels lie within the spin-wave band and can decay into the continuum. It follows that virtual levels can be observed only if the spin-wave density of states at the energies corresponding to these levels is sufficiently small for these levels to be sufficiently long-lived. The spin-wave density of states at the edges of the spectrum is relatively small, so that one can expect fairly narrow virtual levels in this region.

The nature of the impurity levels depends on the symmetry properties of the impurity atom's wave function. In a simple cubic lattice, there may be s, p, and d type modes, in accordance with the irreducible representations of the cubic point group.

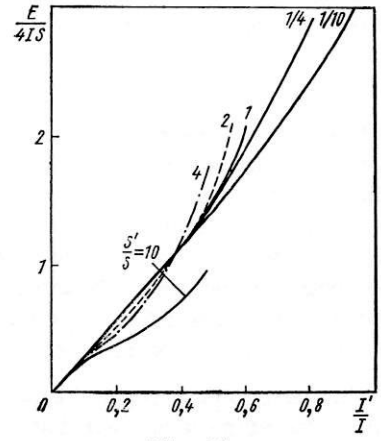

Fig. 18

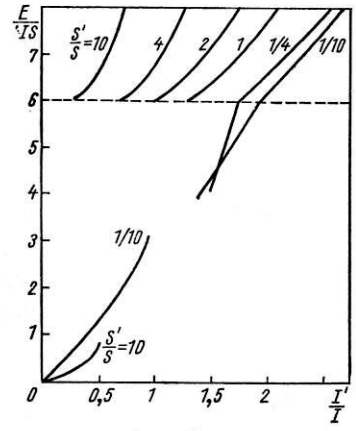

Fig. 19

Fig. 18. Dependence of s-type energy levels on the parameters J'/J and S'/S [9].

Fig. 19. Energy levels of s-type within the spin-wave band and near its upper edge as a function of the parameters J'/J and S'/S [9].

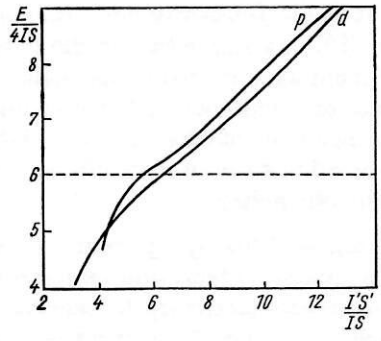

Fig. 20

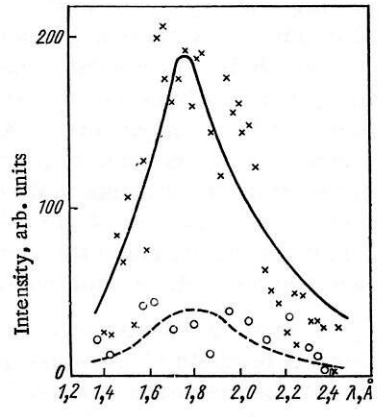

Fig. 21

Fig. 20. Dependence of levels of p and d type on the parameter J'S'/JS [9].

Fig. 21. Virtual level of s-type in Fe(Mn). The continuous curve is the difference between the scattering intensities in the alloy and in the pure iron; the dashed curve is the difference between the scattering intensity in the alloy when there is no external magnetic field and when there is a magnetic field at right angles to the scattering vector.

Since it more convenient to use dimensionless quantities, the energy levels in the diagrams later are expressed in units of 4JS. In these units, for example, the width of the spin-wave band of the matrix is exactly equal to six.

As an illustration we give a typical spin-wave spectrum calculated by Izyumov [9] for a simple cubic lattice with and without impurity atoms. In Fig. 17 the continuous curve corresponds to the spectrum of a perfect lattice; the dashed curve, to a lattice with an impurity. The impurity levels correspond to three different combinations of J'/J and S'/S. If the exchange interaction between the host and impurity atoms is weak and the ratio of the spins is not too large, a narrow virtual level can arise at the bottom of the spin-wave band. Level 1 correspond to these requirements; it is narrow. The other two levels, 2 and 3, are

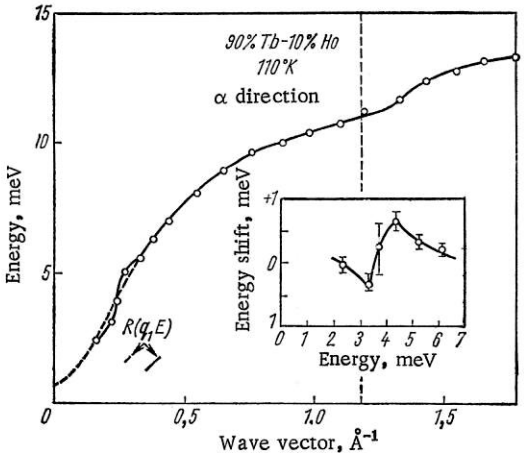

Fig. 22. Dependence of the energy on the wave vector for a Tb single crystal with an admixture of 10% Ho atoms. The small distortion of the dispersion curve is due to the virtual level.

broad because either the ratio of the spins is large or there is a strong interaction between the impurity and the host.

The curves in Fig. 18 illustrate the dependence of the s-type levels on the parameters J'/J and S'/S. Above the bottom of the spin-wave band the energy varies fairly rapidly with increasing spin, but at the bottom of the band the position of the virtual levels does not depend very strongly on the spin ratio. Note that if the exchange integrals ratio is less than 0.1, the energy is virtually independent of the spin ratio. The dependence of the s-type levels on these parameters is shown in Fig. 19.

Virtual levels of p and d type do not exist at the bottom of the spin-wave band, but they may appear near the upper edge of the band when the ratio $J'S'/JS$ is sufficiently large. The energies of these levels are shown as functions of the parameter $J'S'/JS$ in Fig. 20. As the parameter increases, the energy of the levels increases monotonically, and, once the edge of the band has been passed, the levels become localized.

Low-lying excitations of s-type may have great significance for the thermodynamic properties of magnetic crystals at low temperatures. The well-known temperature dependence of the spontaneous magnetization characteristic of pure crystals may be radically altered because an increase in the temperature causes impurity atoms to lose their moment much more rapidly than the host atoms. Low-lying levels have another consequence: an anomaly in the specific heat at low temperatures. Anomalies are also to be expected in transport effects at low temperatures. Kagan [10] has shown that in the temperature region in which the low-lying levels are effective the resistivity must have a broad maximum. Unfortunately, there are only a few macroscopic experiments that confirm the existence of these anomalies. When we come to experiments in which the existence of virtual spin-wave excitations is proved directly, the situation is more favorable. In these experiments the energy-level system of magnetic crystal is measured by means of the well developed methods of slow-neutron spectrometry.

One of the first experiments [11] to indicate the existence of low-lying virtual excitations of s-type was carried out at the Central Institute of Physical Investigations on iron with manganese as an impurity. To obtain direct evidence for the existence of these levels, it was necessary to measure the energy of cold neutrons scattered incoherently by a polycrystalline sample containing 3% manganese atoms. The results are shown in Fig. 21; the lower dashed curve shows that the observed resonance is magnetic in nature; the resonance profile (continuous curve) can be described by a Lorentz function. The energy and the resonance level's width were calculated by the method of least squares with allowance for the profile of the incident neutron spectrum. The energy was found to be 19.8 meV, the width, 6.7 meV. These values made it possible to estimate the ratio of the exchange integrals; it was in the range 0.1-0.2.

However, impurity levels can be studied differently – by analyzing the energy of coherently scattered neutrons. In this case, the energies can be analyzed with a crystal spectrometer. Using this method, Holden et al. [12] were able to observe localized impurity levels in MnF_2 diluted with Co. The virtual levels can be investigated by measuring the small perturbations to the dispersion curve or the spin-waves. Experiments of this kind are rather complicated and cannot be reproduced on samples with low impurity concentration. Mackintosh et al. [13] used a Tb single crystal with a 10% admixture of Ho atoms; they observed a change in the dispersion curve at 4 meV. Figure 22 shows that the change was small. We can conclude that experiments with incoherent scattering of neutrons give more reliable information about virtual levels than coherent scattering experiments because the first can be performed on samples with a fairly low impurity concentration.

High-flux reactors, especially pulsed reactors, will, both now and in the future, be an important means of studying microdisturbances introduced by magnetic impurities in magnetic and nonmagnetic crystals. This is above all because many expected effects of the impurity-matrix interaction can be observed only if

a strong and well-formed neutron beam is available. Since the way to an understanding of disordered systems leads through the correct solution of the problem of an isolated impurity, it is obvious that this very promising branch of modern physics will continue to attract many theoreticians and experimentalists.

LITERATURE CITED

1. G. G. Low, Advances Phys., 18, 371 (1969).
2. G. G. Low, Proc. Phys. Soc., 92, 938 (1967).
3. G. G. Low and M. F. Collins, J. Appl. Phys., 34, 1195 (1963).
4. M. F. Collins and G. G. Low, Proc. Phys. Soc., 86, 535 (1965).
5. A. T. Aldred, J. Phys. C., 1, 244 (1968).
6. I. A. Campbell, Proc. Phys. Soc., 89, 71 (1966).
7. V. Jaccarino, L. R. Walker, and G. K. Wertheim, Phys. Rev., Lett., 13, 752 (1964).
8. T. Wolfram and J. Callaway, Phys. Rev., 130, 2207 (1963).
9. Yu. A. Izyumov and M. V. Medvelev, Zh. Eksp. Teor. Fiz., 49, 1887 (1965).
10. Yu. Kagan and A. P. Zhernov, Zh. Éksp. Teor. Fiz., 50, 1107 (1966).
11. N. Kroo and L. Bata, Phys. Lett., 24, 22 (1967); N. Kroo, L. Pal, and D. Jovic, Neutron Inelastic Scattering, Vol. 11, IAEA, Vienna (1968), p. 37.
12. T. M. Holden, R. A. Cowley, and W. J. L. Buyers, Solid State Communications, 6, 145 (1969).
13. A. R. Mackintosh and H. B. Meller, Proc. Intern. Conf. Localized Excitations, Irvine, California (1967).